Available online at www.sciencedirect.com

SciVerse ScienceDirect

Scripta Materialia 69 (2013) 53–56

Scripta MATERIALIA

www.elsevier.com/locate/scriptamat

Microbanding mechanism in an Fe–Mn–C high-Mn twinning-induced plasticity steel

I. Gutierrez-Urrutia* and D. Raabe

Max-Planck-Institut für Eisenforschung, Max-Planck Str. 1, D-40237 Düsseldorf, Germany

Received 12 February 2013; revised 10 March 2013; accepted 12 March 2013
Available online 19 March 2013

We study the microbanding mechanism in an Fe–22Mn–0.6C (wt.%) twinning-induced plasticity steel. Dislocation substructures were examined by electron channeling contrast imaging and electron backscatter diffraction. We observe a pronounced effect of the strain path on microbanding, which is explained in terms of Schmid's law. Microbands created under shear loading have a non-crystallographic character. This is attributed to the microbanding mechanism and its relation with the dislocation substructure. Further insights into the dislocation configuration of microbands are provided.
© 2013 Acta Materialia Inc. Published by Elsevier Ltd. All rights reserved.

Keywords: Dislocation cell; Plastic deformation; Electron backscattering diffraction (EBSD); Electron channeling contrast imaging (ECCI); Austenitic steels

Recent investigations into the deformation structure in austenitic high-Mn steels, namely, Fe–Mn–C and Fe–Mn–Al–C alloys, have revealed a complex dislocation substructure formed by cells, cell blocks and Taylor lattices [1–6]. These dislocation configurations are formed at low deformation levels (true tensile strain <0.3) and are characterized by characteristic dislocation patterns. Cell blocks and Taylor lattices are delimited by geometrically necessary boundaries (GNBs), referred to as highly dense dislocation walls (HDDWs), and incidental dislocation boundaries (IDB), termed dislocation walls [7,8]. Cells are only defined by IDBs. The underlying mechanisms controlling the formation of dislocation structures are governed by specific dislocation reactions that are stress dependent [9]. Accordingly, dislocation patterning is strongly dependent on the crystallographic orientation [1,2,4]. The role of these dislocation substructures on the strain hardening behavior of high-Mn steels has been addressed recently [1,4]. Specifically, the combination of dislocation substructure hardening (at low and medium true tensile strains, <0.3) together with deformation twinning (at high true tensile strains, >0.3) leads to a multiple-stage strain hardening behavior resulting in permanent strain hardening up to high-deformation regimes and, hence, superior mechanical properties. In addition to these dislocation substructures, high-Mn steels can also develop microbands. These dislocation configurations have been reported in Fe–Mn–Al–C alloys deformed under tension [4,10–12]. Microbands are commonly characterized as paired dense dislocation layers which are separated from each other by a few hundred nanometers. They are associated with a strain localization phenomenon that is characterized by high local dislocation densities [13,14]. Unlike shear bands, which have a non-crystallographic alignment, microbands layers are often aligned with the {1 1 1} slip planes, i.e. they form crystallographic boundaries, and typically remain inside their respective host grains. Microbands may also contribute to the strain-hardening of high-Mn steels, although their specific kinetic role and hardening effects are still unclear [4,10,15]. Therefore, the present study aims at clarifying the microband formation mechanism in high-Mn steels. We have investigated the dislocation substructures, in particular those associated with microbands, obtained under different strain paths, namely, tension and shear, in an Fe–22Mn–0.6C (wt.%) high-Mn twinning-induced plasticity (TWIP) steel by combined electron channeling contrast imaging (ECCI) and electron backscatter diffraction (EBSD). The crystallographic orientation dependences of the dislocation patterns as well as of the dislocation boundary alignments are analyzed. The microband formation mechanism is analyzed in terms of the associated characteristic dislocation configurations.

* Corresponding author. Tel: +49 2116792 407; e-mail: i.gutierrez@mpie.de

1359-6462/$ - see front matter © 2013 Acta Materialia Inc. Published by Elsevier Ltd. All rights reserved.
http://dx.doi.org/10.1016/j.scriptamat.2013.03.010

The high-Mn steel used in this study had the chemical composition Fe–22Mn–0.6C (wt.%). Details on alloy processing can be found in Ref. [1]. The hot-rolled material showed a fully austenitic structure with an average grain size of 50 μm, which remained stable during deformation at room temperature. Tensile and shear tests were carried out at room temperature at an initial strain rate of 5×10^{-4} s^{-1} to an equivalent true strain of 0.1. At this strain level, the deformation structure mainly consists of dislocation substructures with few deformation twins [1]. The tensile bone-shaped samples had a gauge length of 8 mm, a gauge width of 2 mm and a gauge thickness of 1 mm. Shear deformation tests were performed using a shear test set-up described in Ref. [16]. The shear samples had a rectangular shape of dimensions $40 \times 14 \times 2$ mm^3. Dislocation substructures were investigated by combined ECCI and EBSD. Longitudinal sections of the tensile deformed sample, i.e. the section perpendicular to the tensile axis, were examined. In the sample deformed by shear, the shear direction (SD)–normal direction (ND) section was characterized. High-resolution EBSD maps (step size of 50–100 nm) were taken in a 6500 F JEOL field emission gun-scanning electron microscope equipped with a TSL OIM EBSD system. Dislocation substructures of the grains mapped by EBSD were subsequently examined by ECCI under controlled diffraction conditions, as described in previous works [1,3,4,17–19]. ECCI images were obtained with optimum contrast by tilting the matrix crystal into the Bragg condition to obtain high-intensity reflections and to excite the corresponding diffraction vector in a "two-beam" condition. ECCI observations were carried out in a Zeiss Crossbeam instrument (XB 1540, Carl Zeiss SMT AG, Germany) operated at 10 kV.

We examined the dislocation substructures in about 35 individual grains for both tensile- and shear-deformed specimens. Both samples were loaded with an initial strain rate of 5×10^{-4} s^{-1} to an equivalent true strain of 0.1. Substructure analysis was conducted by combined ECCI and EBSD. The experimentally analyzed crystal orientations in the sample deformed under tension are shown in the tensile axis inverse pole figure (TA-IPF) of Figure 1(a). The data provide a good representation of the deformation texture at 0.1 true strain [1]. The dislocation substructure is formed by two types of dislocation patterns, namely, cell blocks (CBs; Fig. 1(b)) and dislocation cells (DCs; Fig. 1(c)). The formation of these dislocation patterns is associated with the multiple character of slip, i.e. wavy and planar [3]. CB is the most common type of dislocation pattern. It is delimited by GNBs (highly-dense dislocation walls, HDDWs) and IDBs, which are also termed dislocation walls [7,8]. These dislocation configurations are imaged by ECCI as bright and compact layers (HDDWs) which are subdivided by finer bright layers (dislocation walls; Fig. 1(b)). CBs are formed in grains oriented along the line between the ⟨001⟩//TA and ⟨111⟩//TA crystallographic directions. Grains oriented close to ⟨112⟩//TA directions develop HDDWs that are parallel within 1°–2° to the {111} plane traces, i.e. they represent crystallographic boundaries. In contrast, grains close to the texture fiber comprising ⟨111⟩//TA directions build up non-crystallographic HDDWs which deviate up to 10° from the {111} slip planes. Equiaxed DCs are built up in grains oriented close to ⟨001⟩//TA directions (Fig. 1(c)). Dislocation substructures similar to those found here have been reported in medium-to-high stacking fault energy metals, such as copper and aluminum, deformed under tension [20,21]. Detailed examination of the dislocation boundaries, in particular of the HDDWs, did not reveal any effect of strain localization on the dislocation patterning such as microbanding.

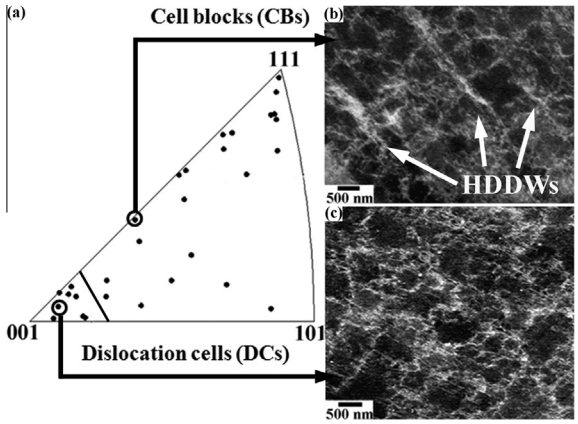

Figure 1. Crystallographic orientation dependence of the dislocation pattern in an Fe–22Mn–0.6C (wt.%) steel tensile deformed to 0.1 true strain. HDDWS: Highly-dense dislocation walls.

Figure 2(a) shows the SD-IPF containing the experimental crystal orientations of the analyzed grains in the sample deformed by shear. The crystals inspected also provide a good representation of the deformation texture at 0.1 equivalent true strain. At this strain level, the dislocation substructure mainly consists of CBs. DCs were observed in only a few grains. Analysis of the dislocation boundary alignment by combined ECCI and EBSD revealed that most of the HDDWs delimiting the CBs are non-crystallographic boundaries, which deviate by up to 10° from the {111} slip planes. Figure 2(b) shows an ECCI image of the CB structure developed in a grain oriented close to the ⟨213⟩//SD direction, where HDDWs are formed almost parallel to the {351} planes. The crystallographic plane trace analysis was carried out by using combined ECCI and EBSD mapping. Detailed examination of the CB structure by ECCI revealed that microbanding is strongly promoted in the sample deformed by shear when compared to the tensile deformed sample. Figure 3(a) shows a high-resolution EBSD map

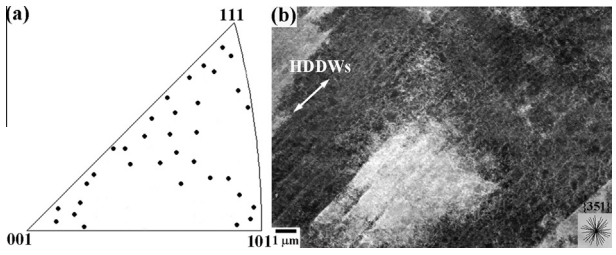

Figure 2. (a) IPF along the shear reference direction showing experimental grain orientations of a sample deformed by shear to 0.1 equivalent true strain. (b) ECCI image of the cell block structure developed in a grain oriented close to ⟨213⟩//SD direction. HDDWs are almost parallel to {351} planes (plane trace analysis was carried out by combined ECCI and EBSD).

Download English Version:

https://daneshyari.com/en/article/1498762

Download Persian Version:

https://daneshyari.com/article/1498762

Daneshyari.com